

Search for the Rare Decays $B \rightarrow K\ell^+\ell^-$ and $B \rightarrow K^*\ell^+\ell^-$

B. Aubert,¹ D. Boutigny,¹ J.-M. Gaillard,¹ A. Hicheur,¹ Y. Karyotakis,¹ J. P. Lees,¹ P. Robbe,¹ V. Tisserand,¹
A. Palano,² A. Pompili,² G. P. Chen,³ J. C. Chen,³ N. D. Qi,³ G. Rong,³ P. Wang,³ Y. S. Zhu,³ G. Eigen,⁴
B. Stugu,⁴ G. S. Abrams,⁵ A. W. Borgland,⁵ A. B. Breon,⁵ D. N. Brown,⁵ J. Button-Shafer,⁵ R. N. Cahn,⁵
A. R. Clark,⁵ M. S. Gill,⁵ A. V. Gritsan,⁵ Y. Groysman,⁵ R. G. Jacobsen,⁵ R. W. Kadel,⁵ J. Kadyk,⁵ L. T. Kerth,⁵
Yu. G. Kolomensky,⁵ J. F. Kral,⁵ C. LeClerc,⁵ M. E. Levi,⁵ G. Lynch,⁵ P. J. Oddone,⁵ M. Pripstein,⁵ N. A. Roe,⁵
A. Romosan,⁵ M. T. Ronan,⁵ V. G. Shelkov,⁵ A. V. Telnov,⁵ W. A. Wenzel,⁵ T. J. Harrison,⁶ C. M. Hawkes,⁶
D. J. Knowles,⁶ S. W. O’Neale,⁶ R. C. Penny,⁶ A. T. Watson,⁶ N. K. Watson,⁶ T. Deppermann,⁷ K. Goetzen,⁷
H. Koch,⁷ M. Kunze,⁷ B. Lewandowski,⁷ K. Peters,⁷ H. Schmoecker,⁷ M. Steinke,⁷ N. R. Barlow,⁸ W. Bhimji,⁸
N. Chevalier,⁸ P. J. Clark,⁸ W. N. Cottingham,⁸ B. Foster,⁸ C. Mackay,⁸ F. F. Wilson,⁸ K. Abe,⁹ C. Hearty,⁹
T. S. Mattison,⁹ J. A. McKenna,⁹ D. Thiessen,⁹ S. Jolly,¹⁰ A. K. McKemey,¹⁰ V. E. Blinov,¹¹ A. D. Bukin,¹¹
D. A. Bukin,¹¹ A. R. Buzykaev,¹¹ V. B. Golubev,¹¹ V. N. Ivanchenko,¹¹ A. A. Korol,¹¹ E. A. Kravchenko,¹¹
A. P. Onuchin,¹¹ S. I. Serednyakov,¹¹ Yu. I. Skovpen,¹¹ V. I. Telnov,¹¹ A. N. Yushkov,¹¹ D. Best,¹² M. Chao,¹²
D. Kirkby,¹² A. J. Lankford,¹² M. Mandelkern,¹² S. McMahon,¹² D. P. Stoker,¹² K. Arisaka,¹³ C. Buchanan,¹³
S. Chun,¹³ D. B. MacFarlane,¹⁴ S. Prell,¹⁴ Sh. Rahatlou,¹⁴ G. Raven,¹⁴ V. Sharma,¹⁴ C. Campagnari,¹⁵
B. Dahmes,¹⁵ P. A. Hart,¹⁵ N. Kuznetsova,¹⁵ S. L. Levy,¹⁵ O. Long,¹⁵ A. Lu,¹⁵ J. D. Richman,¹⁵ W. Verkerke,¹⁵
J. Beringer,¹⁶ A. M. Eisner,¹⁶ M. Grothe,¹⁶ C. A. Heusch,¹⁶ W. S. Lockman,¹⁶ T. Pulliam,¹⁶ T. Schalk,¹⁶
R. E. Schmitz,¹⁶ B. A. Schumm,¹⁶ A. Seiden,¹⁶ M. Turri,¹⁶ W. Walkowiak,¹⁶ D. C. Williams,¹⁶ M. G. Wilson,¹⁶
E. Chen,¹⁷ G. P. Dubois-Felsmann,¹⁷ A. Dvoretzskii,¹⁷ D. G. Hitlin,¹⁷ S. Metzler,¹⁷ J. Oyang,¹⁷ F. C. Porter,¹⁷
A. Ryd,¹⁷ A. Samuel,¹⁷ M. Weaver,¹⁷ S. Yang,¹⁷ R. Y. Zhu,¹⁷ S. Devmal,¹⁸ T. L. Geld,¹⁸ S. Jayatilke,¹⁸
G. Mancinelli,¹⁸ B. T. Meadows,¹⁸ M. D. Sokoloff,¹⁸ T. Barillari,¹⁹ P. Bloom,¹⁹ M. O. Dima,¹⁹ W. T. Ford,¹⁹
U. Nauenberg,¹⁹ A. Olivas,¹⁹ P. Rankin,¹⁹ J. Roy,¹⁹ J. G. Smith,¹⁹ W. C. van Hoek,¹⁹ J. Blouw,²⁰ J. L. Harton,²⁰
M. Krishnamurthy,²⁰ A. Soffer,²⁰ W. H. Toki,²⁰ R. J. Wilson,²⁰ J. Zhang,²⁰ T. Brandt,²¹ J. Brose,²¹
T. Colberg,²¹ M. Dickopp,²¹ R. S. Dubitzky,²¹ A. Hauke,²¹ E. Maly,²¹ R. Müller-Pfefferkorn,²¹ S. Otto,²¹
K. R. Schubert,²¹ R. Schwierz,²¹ B. Spaan,²¹ L. Wilden,²¹ D. Bernard,²² G. R. Bonneaud,²² F. Brochard,²²
J. Cohen-Tanugi,²² S. Ferrag,²² S. T’Jampens,²² Ch. Thiebaux,²² G. Vasileiadis,²² M. Verderi,²² A. Anjomshoaa,²³
R. Bernet,²³ A. Khan,²³ D. Lavin,²³ F. Muheim,²³ S. Playfer,²³ J. E. Swain,²³ J. Tinslay,²³ M. Falbo,²⁴
C. Borean,²⁵ C. Bozzi,²⁵ S. Dittongo,²⁵ L. Piemontese,²⁵ E. Treadwell,²⁶ F. Anulli,²⁷ * R. Baldini-Ferrolì,²⁷
A. Calcaterra,²⁷ R. de Sangro,²⁷ D. Falciai,²⁷ G. Finocchiaro,²⁷ P. Patteri,²⁷ I. M. Peruzzi,²⁷ * M. Piccolo,²⁷
Y. Xie,²⁷ A. Zallo,²⁷ S. Bagnasco,²⁸ A. Buzzo,²⁸ R. Contri,²⁸ G. Crosetti,²⁸ M. Lo Vetere,²⁸ M. Macri,²⁸
M. R. Monge,²⁸ S. Passaggio,²⁸ F. C. Pastore,²⁸ C. Patrignani,²⁸ M. G. Pia,²⁸ E. Robutti,²⁸ A. Santroni,²⁸
S. Tosi,²⁸ M. Morii,²⁹ R. Bartoldus,³⁰ R. Hamilton,³⁰ U. Mallik,³⁰ J. Cochran,³¹ H. B. Crawley,³¹ P.-A. Fischer,³¹
J. Lamsa,³¹ W. T. Meyer,³¹ E. I. Rosenberg,³¹ G. Grosdidier,³² C. Hast,³² A. Höcker,³² H. M. Lacker,³²
S. Laplace,³² V. Lepeltier,³² A. M. Lutz,³² S. Plaszczynski,³² M. H. Schune,³² S. Trincz-Duvold,³² G. Wormser,³²
R. M. Bionta,³³ V. Brigljević,³³ D. J. Lange,³³ M. Mugge,³³ K. van Bibber,³³ D. M. Wright,³³ A. J. Bevan,³⁴
J. R. Fry,³⁴ E. Gabathuler,³⁴ R. Gamet,³⁴ M. George,³⁴ M. Kay,³⁴ D. J. Payne,³⁴ R. J. Sloane,³⁴ C. Touramanis,³⁴
M. L. Aspinwall,³⁵ D. A. Bowerman,³⁵ P. D. Dauncey,³⁵ U. Egede,³⁵ I. Eschrich,³⁵ N. J. W. Gunawardane,³⁵
J. A. Nash,³⁵ P. Sanders,³⁵ D. Smith,³⁵ D. E. Azzopardi,³⁶ J. J. Back,³⁶ G. Bellodi,³⁶ P. Dixon,³⁶ P. F. Harrison,³⁶
R. J. L. Potter,³⁶ H. W. Shorthouse,³⁶ P. Strother,³⁶ P. B. Vidal,³⁶ G. Cowan,³⁷ S. George,³⁷ M. G. Green,³⁷
A. Kurup,³⁷ C. E. Marker,³⁷ P. McGrath,³⁷ T. R. McMahon,³⁷ S. Ricciardi,³⁷ F. Salvatore,³⁷ G. Vaitsas,³⁷
D. Brown,³⁸ C. L. Davis,³⁸ J. Allison,³⁹ R. J. Barlow,³⁹ J. T. Boyd,³⁹ A. C. Forti,³⁹ J. Fullwood,³⁹ F. Jackson,³⁹
G. D. Lafferty,³⁹ N. Savvas,³⁹ J. H. Weatherall,³⁹ J. C. Williams,³⁹ A. Farbin,⁴⁰ A. Jawahery,⁴⁰ V. Lillard,⁴⁰
J. Olsen,⁴⁰ D. A. Roberts,⁴⁰ J. R. Schieck,⁴⁰ G. Blaylock,⁴¹ C. Dallapiccola,⁴¹ K. T. Flood,⁴¹ S. S. Hertzbach,⁴¹
R. Kofler,⁴¹ V. B. Koptchev,⁴¹ T. B. Moore,⁴¹ H. Staengle,⁴¹ S. Willocq,⁴¹ B. Brau,⁴² R. Cowan,⁴² G. Sciolla,⁴²
F. Taylor,⁴² R. K. Yamamoto,⁴² M. Milek,⁴³ P. M. Patel,⁴³ F. Palombo,⁴⁴ J. M. Bauer,⁴⁵ L. Cremaldi,⁴⁵
V. Eschenburg,⁴⁵ R. Kroeger,⁴⁵ J. Reidy,⁴⁵ D. A. Sanders,⁴⁵ D. J. Summers,⁴⁵ J. Y. Nief,⁴⁶ P. Taras,⁴⁶

H. Nicholson,⁴⁷ C. Cartaro,⁴⁸ N. Cavallo,^{48,†} G. De Nardo,⁴⁸ F. Fabozzi,⁴⁸ C. Gatto,⁴⁸ L. Lista,⁴⁸ P. Paolucci,⁴⁸
D. Piccolo,⁴⁸ C. Sciacca,⁴⁸ J. M. LoSecco,⁴⁹ J. R. G. Alsmiller,⁵⁰ T. A. Gabriel,⁵⁰ J. Brau,⁵¹ R. Frey,⁵¹
E. Grauges,⁵¹ M. Iwasaki,⁵¹ N. B. Sinev,⁵¹ D. Strom,⁵¹ F. Colecchia,⁵² F. Dal Corso,⁵² A. Dorigo,⁵² F. Galeazzi,⁵²
M. Margoni,⁵² G. Michelon,⁵² M. Morandin,⁵² M. Posocco,⁵² M. Rotondo,⁵² F. Simonetto,⁵² R. Stroili,⁵²
E. Torassa,⁵² C. Voci,⁵² M. Benayoun,⁵³ H. Briand,⁵³ J. Chauveau,⁵³ P. David,⁵³ Ch. de la Vaissière,⁵³ L. Del
Buono,⁵³ O. Hamon,⁵³ F. Le Diberder,⁵³ Ph. Leruste,⁵³ J. Ocariz,⁵³ L. Roos,⁵³ J. Stark,⁵³ P. F. Manfredi,⁵⁴
V. Re,⁵⁴ V. Speziali,⁵⁴ E. D. Frank,⁵⁵ L. Gladney,⁵⁵ Q. H. Guo,⁵⁵ J. Panetta,⁵⁵ C. Angelini,⁵⁶ G. Batignani,⁵⁶
S. Bettarini,⁵⁶ M. Bondioli,⁵⁶ F. Bucci,⁵⁶ E. Campagna,⁵⁶ M. Carpinelli,⁵⁶ F. Forti,⁵⁶ M. A. Giorgi,⁵⁶ A. Lusiani,⁵⁶
G. Marchiori,⁵⁶ F. Martinez-Vidal,⁵⁶ M. Morganti,⁵⁶ N. Neri,⁵⁶ E. Paoloni,⁵⁶ M. Rama,⁵⁶ G. Rizzo,⁵⁶ F. Sandrelli,⁵⁶
G. Simi,⁵⁶ G. Triggiani,⁵⁶ J. Walsh,⁵⁶ M. Haire,⁵⁷ D. Judd,⁵⁷ K. Paick,⁵⁷ L. Turnbull,⁵⁷ D. E. Wagoner,⁵⁷
J. Albert,⁵⁸ P. Elmer,⁵⁸ C. Lu,⁵⁸ V. Miftakov,⁵⁸ S. F. Schaffner,⁵⁸ A. J. S. Smith,⁵⁸ A. Tumanov,⁵⁸ E. W. Varnes,⁵⁸
G. Cavoto,⁵⁹ D. del Re,⁵⁹ R. Faccini,^{14,59} F. Ferrarotto,⁵⁹ F. Ferroni,⁵⁹ E. Lamanna,⁵⁹ M. A. Mazzoni,⁵⁹
S. Morganti,⁵⁹ G. Piredda,⁵⁹ F. Safai Tehrani,⁵⁹ M. Serra,⁵⁹ C. Voena,⁵⁹ S. Christ,⁶⁰ R. Waldi,⁶⁰ T. Adye,⁶¹
N. De Groot,⁶¹ B. Franek,⁶¹ N. I. Geddes,⁶¹ G. P. Gopal,⁶¹ S. M. Xella,⁶¹ R. Aleksan,⁶² S. Emery,⁶²
A. Gaidot,⁶² S. F. Ganzhur,⁶² P.-F. Giraud,⁶² G. Hamel de Monchenault,⁶² W. Kozanecki,⁶² M. Langer,⁶²
G. W. London,⁶² B. Mayer,⁶² B. Serfass,⁶² G. Vasseur,⁶² Ch. Yèche,⁶² M. Zito,⁶² M. V. Purohit,⁶³ H. Singh,⁶³
A. W. Weidemann,⁶³ F. X. Yumiceva,⁶³ I. Adam,⁶⁴ D. Aston,⁶⁴ N. Berger,⁶⁴ A. M. Boyarski,⁶⁴ G. Calderini,⁶⁴
M. R. Convery,⁶⁴ D. P. Coupal,⁶⁴ D. Dong,⁶⁴ J. Dorfan,⁶⁴ W. Dunwoodie,⁶⁴ R. C. Field,⁶⁴ T. Glanzman,⁶⁴
S. J. Gowdy,⁶⁴ T. Haas,⁶⁴ T. Himel,⁶⁴ T. Hryn'ova,⁶⁴ M. E. Huffer,⁶⁴ W. R. Innes,⁶⁴ C. P. Jessop,⁶⁴
M. H. Kelsey,⁶⁴ P. Kim,⁶⁴ M. L. Kocian,⁶⁴ U. Langenegger,⁶⁴ D. W. G. S. Leith,⁶⁴ S. Luitz,⁶⁴ V. Luth,⁶⁴
H. L. Lynch,⁶⁴ H. Marsiske,⁶⁴ S. Menke,⁶⁴ R. Messner,⁶⁴ D. R. Muller,⁶⁴ C. P. O'Grady,⁶⁴ V. E. Ozcan,⁶⁴
A. Perazzo,⁶⁴ M. Perl,⁶⁴ S. Petrak,⁶⁴ H. Quinn,⁶⁴ B. N. Ratcliff,⁶⁴ S. H. Robertson,⁶⁴ A. Roodman,⁶⁴
A. A. Salnikov,⁶⁴ T. Schietinger,⁶⁴ R. H. Schindler,⁶⁴ J. Schwiening,⁶⁴ A. Snyder,⁶⁴ A. Soha,⁶⁴ S. M. Spanier,⁶⁴
J. Stelzer,⁶⁴ D. Su,⁶⁴ M. K. Sullivan,⁶⁴ H. A. Tanaka,⁶⁴ J. Va'vra,⁶⁴ S. R. Wagner,⁶⁴ A. J. R. Weinstein,⁶⁴
W. J. Wisniewski,⁶⁴ D. H. Wright,⁶⁴ C. C. Young,⁶⁴ P. R. Burchat,⁶⁵ C. H. Cheng,⁶⁵ T. I. Meyer,⁶⁵ C. Roat,⁶⁵
R. Henderson,⁶⁶ W. Bugg,⁶⁷ H. Cohn,⁶⁷ J. M. Izen,⁶⁸ I. Kitayama,⁶⁸ X. C. Lou,⁶⁸ F. Bianchi,⁶⁹ M. Bona,⁶⁹
D. Gamba,⁶⁹ L. Bosio,⁷⁰ G. Della Ricca,⁷⁰ L. Lanceri,⁷⁰ P. Poropat,⁷⁰ G. Vuagnin,⁷⁰ R. S. Panvini,⁷¹
C. M. Brown,⁷² P. D. Jackson,⁷² R. Kowalewski,⁷² J. M. Roney,⁷² H. R. Band,⁷³ E. Charles,⁷³ S. Dasu,⁷³
A. M. Eichenbaum,⁷³ H. Hu,⁷³ J. R. Johnson,⁷³ R. Liu,⁷³ F. Di Lodovico,⁷³ Y. Pan,⁷³ R. Prepost,⁷³ I. J. Scott,⁷³
S. J. Sekula,⁷³ J. H. von Wimmersperg-Toeller,⁷³ S. L. Wu,⁷³ Z. Yu,⁷³ T. M. B. Kordich,⁷⁴ and H. Neal⁷⁴

(The BABAR Collaboration)

¹Laboratoire de Physique des Particules, F-74941 Annecy-le-Vieux, France

²Università di Bari, Dipartimento di Fisica and INFN, I-70126 Bari, Italy

³Institute of High Energy Physics, Beijing 100039, China

⁴University of Bergen, Inst. of Physics, N-5007 Bergen, Norway

⁵Lawrence Berkeley National Laboratory and University of California, Berkeley, CA 94720, USA

⁶University of Birmingham, Birmingham, B15 2TT, United Kingdom

⁷Ruhr Universität Bochum, Institut für Experimentalphysik 1, D-44780 Bochum, Germany

⁸University of Bristol, Bristol BS8 1TL, United Kingdom

⁹University of British Columbia, Vancouver, BC, Canada V6T 1Z1

¹⁰Brunel University, Uxbridge, Middlesex UB8 3PH, United Kingdom

¹¹Budker Institute of Nuclear Physics, Novosibirsk 630090, Russia

¹²University of California at Irvine, Irvine, CA 92697, USA

¹³University of California at Los Angeles, Los Angeles, CA 90024, USA

¹⁴University of California at San Diego, La Jolla, CA 92093, USA

¹⁵University of California at Santa Barbara, Santa Barbara, CA 93106, USA

¹⁶University of California at Santa Cruz, Institute for Particle Physics, Santa Cruz, CA 95064, USA

¹⁷California Institute of Technology, Pasadena, CA 91125, USA

¹⁸University of Cincinnati, Cincinnati, OH 45221, USA

¹⁹University of Colorado, Boulder, CO 80309, USA

²⁰Colorado State University, Fort Collins, CO 80523, USA

²¹Technische Universität Dresden, Institut für Kern- und Teilchenphysik, D-01062 Dresden, Germany

²²Ecole Polytechnique, F-91128 Palaiseau, France

²³University of Edinburgh, Edinburgh EH9 3JZ, United Kingdom

²⁴Elon University, Elon University, NC 27244-2010, USA

²⁵Università di Ferrara, Dipartimento di Fisica and INFN, I-44100 Ferrara, Italy

- ²⁶Florida A&M University, Tallahassee, FL 32307, USA
²⁷Laboratori Nazionali di Frascati dell'INFN, I-00044 Frascati, Italy
²⁸Università di Genova, Dipartimento di Fisica and INFN, I-16146 Genova, Italy
²⁹Harvard University, Cambridge, MA 02138, USA
³⁰University of Iowa, Iowa City, IA 52242, USA
³¹Iowa State University, Ames, IA 50011-3160, USA
³²Laboratoire de l'Accélérateur Linéaire, F-91898 Orsay, France
³³Lawrence Livermore National Laboratory, Livermore, CA 94550, USA
³⁴University of Liverpool, Liverpool L69 3BX, United Kingdom
³⁵University of London, Imperial College, London, SW7 2BW, United Kingdom
³⁶Queen Mary, University of London, E1 4NS, United Kingdom
³⁷University of London, Royal Holloway and Bedford New College, Egham, Surrey TW20 0EX, United Kingdom
³⁸University of Louisville, Louisville, KY 40292, USA
³⁹University of Manchester, Manchester M13 9PL, United Kingdom
⁴⁰University of Maryland, College Park, MD 20742, USA
⁴¹University of Massachusetts, Amherst, MA 01003, USA
⁴²Massachusetts Institute of Technology, Laboratory for Nuclear Science, Cambridge, MA 02139, USA
⁴³McGill University, Montréal, QC, Canada H3A 2T8
⁴⁴Università di Milano, Dipartimento di Fisica and INFN, I-20133 Milano, Italy
⁴⁵University of Mississippi, University, MS 38677, USA
⁴⁶Université de Montréal, Laboratoire René J. A. Lévesque, Montréal, QC, Canada H3C 3J7
⁴⁷Mount Holyoke College, South Hadley, MA 01075, USA
⁴⁸Università di Napoli Federico II, Dipartimento di Scienze Fisiche and INFN, I-80126, Napoli, Italy
⁴⁹University of Notre Dame, Notre Dame, IN 46556, USA
⁵⁰Oak Ridge National Laboratory, Oak Ridge, TN 37831, USA
⁵¹University of Oregon, Eugene, OR 97403, USA
⁵²Università di Padova, Dipartimento di Fisica and INFN, I-35131 Padova, Italy
⁵³Universités Paris VI et VII, Lab de Physique Nucléaire H. E., F-75252 Paris, France
⁵⁴Università di Pavia, Dipartimento di Elettronica and INFN, I-27100 Pavia, Italy
⁵⁵University of Pennsylvania, Philadelphia, PA 19104, USA
⁵⁶Università di Pisa, Scuola Normale Superiore and INFN, I-56010 Pisa, Italy
⁵⁷Prairie View A&M University, Prairie View, TX 77446, USA
⁵⁸Princeton University, Princeton, NJ 08544, USA
⁵⁹Università di Roma La Sapienza, Dipartimento di Fisica and INFN, I-00185 Roma, Italy
⁶⁰Universität Rostock, D-18051 Rostock, Germany
⁶¹Rutherford Appleton Laboratory, Chilton, Didcot, Oxon, OX11 0QX, United Kingdom
⁶²DAPNIA, Commissariat à l'Energie Atomique/Saclay, F-91191 Gif-sur-Yvette, France
⁶³University of South Carolina, Columbia, SC 29208, USA
⁶⁴Stanford Linear Accelerator Center, Stanford, CA 94309, USA
⁶⁵Stanford University, Stanford, CA 94305-4060, USA
⁶⁶TRIUMF, Vancouver, BC, Canada V6T 2A3
⁶⁷University of Tennessee, Knoxville, TN 37996, USA
⁶⁸University of Texas at Dallas, Richardson, TX 75083, USA
⁶⁹Università di Torino, Dipartimento di Fisica Sperimentale and INFN, I-10125 Torino, Italy
⁷⁰Università di Trieste, Dipartimento di Fisica and INFN, I-34127 Trieste, Italy
⁷¹Vanderbilt University, Nashville, TN 37235, USA
⁷²University of Victoria, Victoria, BC, Canada V8W 3P6
⁷³University of Wisconsin, Madison, WI 53706, USA
⁷⁴Yale University, New Haven, CT 06511, USA

(Dated: January 4, 2002)

We present results from a search for the flavor-changing neutral current decays $B \rightarrow K\ell^+\ell^-$ and $B \rightarrow K^*\ell^+\ell^-$, where $\ell^+\ell^-$ is either an e^+e^- or $\mu^+\mu^-$ pair. The data sample comprises 22.7×10^6 $\Upsilon(4S) \rightarrow B\bar{B}$ decays collected with the BABAR detector at the PEP-II B Factory. We obtain the 90% C.L. upper limits $\mathcal{B}(B \rightarrow K\ell^+\ell^-) < 0.50 \times 10^{-6}$ and $\mathcal{B}(B \rightarrow K^*\ell^+\ell^-) < 2.9 \times 10^{-6}$, close to Standard Model predictions for these branching fractions. We have also obtained limits on the lepton-family-violating decays $B \rightarrow Ke^\pm\mu^\mp$ and $B \rightarrow K^*e^\pm\mu^\mp$.

PACS numbers: 13.25.Hw, 13.20.He

The flavor-changing neutral current decays $B \rightarrow K\ell^+\ell^-$ and $B \rightarrow K^*(892)\ell^+\ell^-$, where ℓ^\pm is a charged lepton, are highly suppressed in the Standard Model,

with branching fractions predicted to be of order $10^{-7} - 10^{-6}$ [1, 2]. The dominant contributions arise at the one-loop level and are known as electroweak penguins.

Besides probing Standard Model loop effects, these rare decays are important because their rates and kinematic distributions are sensitive to new, heavy particles—such as those predicted by supersymmetric models—that can appear virtually in the loop [1, 2].

The Standard Model predictions for $B \rightarrow K^{(*)}\ell^+\ell^-$ include three main contributions: the electromagnetic (EM) penguin, the Z penguin, and the W^+W^- box diagram. Evidence for the EM penguin amplitude has been obtained from the observation of $B \rightarrow K^*\gamma$ and inclusive $B \rightarrow X_s\gamma$, where X_s is any hadronic system with strangeness [3, 4].

Calculations of decay rates for $B \rightarrow K^{(*)}\ell^+\ell^-$ based on the Standard Model have significant uncertainties due to strong interactions. For example, Ali *et al.* [1] predict $\mathcal{B}(B \rightarrow K\ell^+\ell^-) = (0.57^{+0.17}_{-0.10}) \times 10^{-6}$ for both e^+e^- and $\mu^+\mu^-$ final states, $\mathcal{B}(B \rightarrow K^*e^+e^-) = (2.3^{+0.7}_{-0.5}) \times 10^{-6}$, and $\mathcal{B}(B \rightarrow K^*\mu^+\mu^-) = (1.9^{+0.5}_{-0.4}) \times 10^{-6}$. The contribution of the EM penguin amplitude to $B \rightarrow K^*\ell^+\ell^-$ is particularly strong at low values of $m_{\ell^+\ell^-}$, giving a larger rate for $B \rightarrow K^*e^+e^-$ than for $B \rightarrow K^*\mu^+\mu^-$.

We search for the following decays: $B^+ \rightarrow K^+\ell^+\ell^-$, $B^0 \rightarrow K_S^0\ell^+\ell^-$, $B^+ \rightarrow K^{*+}\ell^+\ell^-$, and $B^0 \rightarrow K^{*0}\ell^+\ell^-$, where $K^{*0} \rightarrow K^+\pi^-$, $K^{*+} \rightarrow K_S^0\pi^+$, $K_S^0 \rightarrow \pi^+\pi^-$, and ℓ is either an e or μ . We also search for the lepton-family-violating decays $B \rightarrow K^{(*)}e^\pm\mu^\mp$. Throughout this paper, charge-conjugate modes are implied.

The data used in the analysis were collected with the BABAR detector at the PEP-II storage ring at the Stanford Linear Accelerator Center during 1999–2000. We analyzed a 20.7 fb^{-1} data sample taken on the $\Upsilon(4S)$ resonance consisting of $(22.7 \pm 0.4) \times 10^6$ $\Upsilon(4S) \rightarrow B\bar{B}$ events.

This search relies primarily on the charged-particle tracking and particle-identification capabilities of the BABAR detector [5]. Charged particle tracking is provided by a five-layer silicon vertex tracker (SVT) and a 40-layer drift chamber (DCH). The DIRC, a Cherenkov ring-imaging particle-identification system, is used for charged hadron identification. Electrons are identified using the electromagnetic calorimeter (EMC), which comprises 6580 thallium-doped CsI crystals. These systems are mounted inside a 1.5 T solenoidal superconducting magnet. Muons are identified in the instrumented flux return (IFR), in which resistive plate chambers are interleaved with the iron plates of the magnet flux return.

We extract the signal using the kinematic variables $m_{\text{ES}} = \sqrt{E_b^{*2} - (\sum_i \mathbf{p}_i^*)^2}$ and $\Delta E = \sum_i \sqrt{m_i^2 + \mathbf{p}_i^{*2}} - E_b^*$, where E_b^* is the beam energy in the e^+e^- rest (c.m.) frame, \mathbf{p}_i^* is the c.m. momentum of daughter particle i in the B meson candidate, and m_i is the mass of particle i . For signal events, m_{ES} peaks at the B meson mass with a resolution of about $2.5 \text{ MeV}/c^2$ and ΔE peaks near zero, indicating that the candidate system of particles has total energy consistent with the beam energy in the c.m. frame.

To prevent bias in the analysis, we optimized the event-selection criteria using Monte Carlo samples: we did not look at the data in the signal region or in the sidebands that were used to measure the background until these criteria were fixed. Signal efficiencies were determined using the Ali *et al.* model [1].

We select events that have at least four charged tracks, the ratio R_2 of the second and zeroth Fox-Wolfram moments [6] less than 0.5, and two oppositely charged leptons with momentum $p > 0.5$ (1.0) GeV/c for e (μ) candidates. Electron-positron pairs consistent with photon conversions in the detector material are vetoed. We require charged kaon candidates to be identified as kaons and the charged pion in $K^* \rightarrow K\pi$ not to be identified as a kaon. For $B \rightarrow K^*\ell^+\ell^-$, we require the mass of the K^* candidate to be within $75 \text{ MeV}/c^2$ of the mean $K^*(892)$ mass. K_S^0 candidates are reconstructed from two oppositely charged tracks that form a good vertex displaced from the primary vertex by at least 1 mm.

The decays $B \rightarrow J/\psi(\rightarrow \ell^+\ell^-)K^{(*)}$ and $B \rightarrow \psi(2S)(\rightarrow \ell^+\ell^-)K^{(*)}$ have identical topologies to signal events. These backgrounds are suppressed by applying a veto in the ΔE vs. $m_{\ell^+\ell^-}$ plane (Fig. 1). This veto removes charmonium events not only with reconstructed $m_{\ell^+\ell^-}$ values near the nominal charmonium masses, but also events that lie further away in $m_{\ell^+\ell^-}$ due to photon radiation (more pronounced in electron channels) or track mismeasurement. Removing all of these events simplifies the description of the background shape. Charmonium events can, however, pass this veto if one of the leptons (typically a muon) and the kaon are misidentified as each other. If reassignment of particle types results in a dilepton mass consistent with the J/ψ or $\psi(2S)$ mass, the candidate is vetoed. There is also significant feed-up from $B \rightarrow J/\psi K$ and $B \rightarrow \psi(2S)K$ into $B \rightarrow K^*\ell^+\ell^-$, since energy lost due to bremsstrahlung in $B \rightarrow J/\psi K$ can be compensated for by including a random pion. If the $K\ell^+\ell^-$ system in a $B \rightarrow K^*\ell^+\ell^-$ candidate is kinematically consistent with $B \rightarrow J/\psi(\rightarrow \ell^+\ell^-\gamma)K$, assuming that the photon (which is not directly observed) was radiated along the direction of either lepton, then the candidate is vetoed. Apart from the charmonium vetoes, we analyze the full $m_{\ell^+\ell^-}$ range.

Continuum background from non-resonant $e^+e^- \rightarrow q\bar{q}$ production is suppressed using a Fisher discriminant [7], a linear combination of the input variables with optimized coefficients. The variables are R_2 ; $\cos\theta_B$, the cosine of the angle between the B candidate and the beam axis in the c.m. frame; $\cos\theta_T$, the cosine of the angle between the thrust axis of the candidate B meson daughter particles and that of the rest of the particles in the c.m. frame; and $m_{K\ell}$, the invariant mass of the K -lepton system, where the lepton is selected according to its charge relative to the strangeness of the $K^{(*)}$. The variable $m_{K\ell}$ helps discriminate against background from

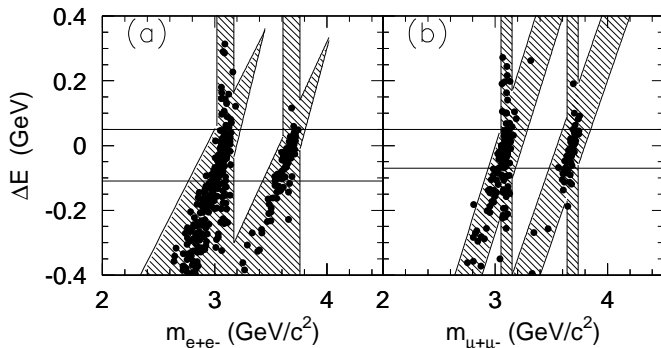


FIG. 1: Charmonium veto in the ΔE vs. $m_{\ell^+\ell^-}$ plane for (a) $B \rightarrow K^{(*)}e^+e^-$ and (b) $B \rightarrow K^{(*)}\mu^+\mu^-$. Hatched regions are vetoed. The dots correspond to a Monte Carlo simulation of $B \rightarrow J/\psi(\rightarrow \ell^+\ell^-)K$ and $B \rightarrow \psi(2S)(\rightarrow \ell^+\ell^-)K$. Most signal events would lie in the ΔE region between the horizontal lines.

semileptonic D decays, for which $m_{K\ell} < m_D$.

Combinatorial background from $B\bar{B}$ events is suppressed using a signal-to- $B\bar{B}$ likelihood ratio that combines candidate B and dilepton vertex probabilities; the significance of the dilepton separation along the beam direction; $\cos\theta_B$; and the missing energy, E_{miss} , of the event in the c.m. frame. The variable E_{miss} provides the strongest discrimination against $B\bar{B}$ background, since events with semileptonic decays usually have significant unobserved energy due to neutrinos. For each final state, we select at most one combination of particles per event as a B signal candidate. If multiple candidates occur, we select the candidate with the greatest number of drift chamber and SVT hits on the charged tracks.

We use the known charmonium decays $B \rightarrow J/\psi K^{(*)}$ and $B \rightarrow \psi(2S)K^{(*)}$ to check the efficiency of our analysis cuts. Figure 2 compares the ΔE distributions (absolutely normalized) of these charmonium samples in Monte Carlo with data. We find good agreement in both the normalization and the shape.

We extract the signal and background yields in each channel using a two-dimensional extended unbinned maximum likelihood fit in the region defined by $m_{\text{ES}} > 5.2 \text{ GeV}/c^2$ and $|\Delta E| < 0.25 \text{ GeV}$. The signal shapes, including the effects of radiation on the ΔE distribution and the correlation between m_{ES} and ΔE , are obtained by parametrizing the GEANT3 Monte Carlo [8] simulation of the signal. The background is described by a function [9] with two parameters that are determined in our fits to the data. Backgrounds from $B\bar{B}$ that peak in the signal region are suppressed to less than 0.2 events in each mode. Although we allow the signal yield to be negative, we have imposed a lower cut-off such that the total fit function is positive. The fit results are shown in Fig. 3 and summarized in Table I. We observe no significant signals.

To determine 90% C.L. upper limits on the signal

yields, we generate and fit a series of toy Monte Carlo samples in which the background probability density function is taken from our fit to the data, but the mean number of signal events is varied. We generate ten thousand samples for each mean value, increasing the mean until 90% of the fits to a set of samples give a signal yield greater than that obtained by fitting the data. To give a measure of the sensitivity of the analysis we list in Table I an effective background yield. This quantity is defined as the square of the error on the signal yield from a fit to a toy Monte Carlo sample drawn from the background probability function, with no signal contribution.

Table I lists the systematic uncertainties from the fit, $(\Delta\mathcal{B}/\mathcal{B})_{\text{fit}}$, expressed according to their effect on the limits. The sensitivity of the limits to the values used for signal-shape parameters is determined by performing alternative fits using parameters from the $B \rightarrow J/\psi K^{(*)}$ control samples. For modes with electrons, we also varied the fraction of signal events in the tail of the ΔE distribution. To determine whether a more general background shape would lead to different results, we introduced additional parameters and allowed for a correlation between m_{ES} and ΔE . This procedure shifted the upper limits by 2% to 5%, depending on the mode. Most of the uncertainty associated with the background shape is incorporated in the statistical error on the yield because the background shape is determined from the fit.

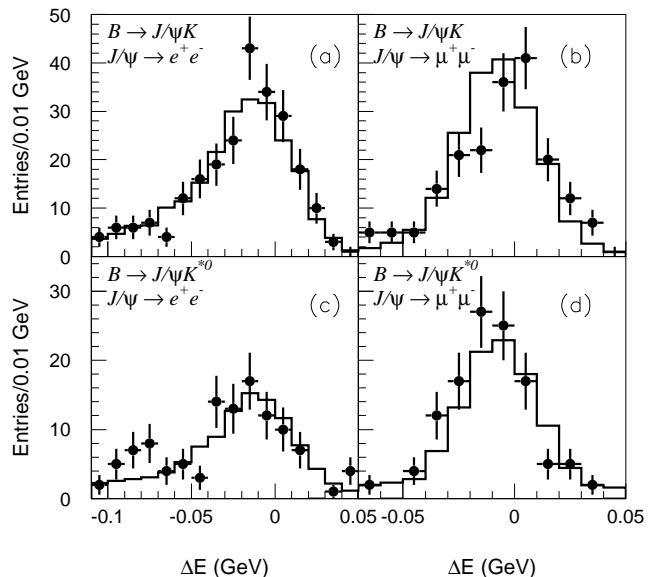


FIG. 2: Comparison of event yields and ΔE shapes between data and Monte Carlo for the charmonium control samples. The points with error bars show the data, and the solid histograms show the prediction of the charmonium Monte Carlo. All of the analysis selection criteria have been applied except for the charmonium veto, which is reversed. The large tails in the e^+e^- modes are due to photon radiation. Small shifts between data and Monte Carlo are taken into account as systematic uncertainties on the signal yields.

TABLE I: Results from the fits to $B \rightarrow K^{(*)}\ell^+\ell^-$ and $B \rightarrow K^{(*)}e^\pm\mu^\mp$ modes. The columns from left to right are fitted signal yield [10]; upper limit on the signal yield; the contribution of the background to the error on the signal yield, expressed as an effective background yield (see text); the signal efficiency, ϵ (not including the branching fractions for K^* , K^0 , and K_S^0 decays); the systematic error on the selection efficiency, $(\Delta\mathcal{B}/\mathcal{B})_\epsilon$; the systematic error from the fit, $(\Delta\mathcal{B}/\mathcal{B})_{\text{fit}}$; the branching fraction central value (\mathcal{B}); and the upper limit on the branching fraction, including systematic errors.

Mode	Signal yield	90% C.L. yield	Effective background	ϵ (%)	$(\Delta\mathcal{B}/\mathcal{B})_\epsilon$ (%)	$(\Delta\mathcal{B}/\mathcal{B})_{\text{fit}}$ (%)	$\mathcal{B}/10^{-6}$	$\mathcal{B}/10^{-6}$ 90% C.L.
$B^+ \rightarrow K^+e^+e^-$	$-0.2^{+1.5}_{-0.0}$	3.1	0.7	17.5	± 7.6	± 4.0	$0.0^{+0.4}_{-0.0}$	0.8
$B^+ \rightarrow K^+\mu^+\mu^-$	$-0.3^{+1.3}_{-0.0}$	2.6	0.6	10.5	± 7.5	± 4.0	$-0.1^{+0.5}_{-0.0}$	1.2
$B^0 \rightarrow K^{*0}e^+e^-$	$3.8^{+3.8}_{-2.1}$	8.8	1.4	10.2	± 8.8	± 11.9	$2.5^{+2.5}_{-1.4}$	6.6
$B^0 \rightarrow K^{*0}\mu^+\mu^-$	$-0.3^{+1.7}_{-0.0}$	3.5	0.7	8.0	± 10.8	± 3.0	$-0.2^{+1.4}_{-0.0}$	3.2
$B^0 \rightarrow K^0e^+e^-$	$1.1^{+2.7}_{-0.9}$	4.2	0.2	15.7	± 8.8	± 9.5	$0.9^{+2.2}_{-0.8}$	3.9
$B^0 \rightarrow K^0\mu^+\mu^-$	$0.0^{+1.2}_{-0.0}$	2.5	0.1	9.6	± 8.8	± 3.0	$0.0^{+1.6}_{-0.0}$	3.7
$B^+ \rightarrow K^{*+}e^+e^-$	$-0.4^{+1.9}_{-1.0}$	3.8	1.6	8.5	± 11.0	± 5.0	$-0.8^{+4.3}_{-0.0}$	9.6
$B^+ \rightarrow K^{*+}\mu^+\mu^-$	$1.2^{+2.4}_{-1.0}$	4.5	0.3	5.8	± 13.0	± 7.6	$3.9^{+8.1}_{-3.2}$	17.3
$B^+ \rightarrow K^+e^\pm\mu^\mp$	$-0.4^{+1.4}_{-0.0}$	2.9	1.3	16.8	± 5.7	± 4.0	$-0.1^{+0.4}_{-0.0}$	0.8
$B^0 \rightarrow K^{*0}e^\pm\mu^\mp$	$1.1^{+3.3}_{-1.6}$	5.3	2.7	11.9	± 7.1	± 10.4	$0.6^{+1.8}_{-0.9}$	3.3
$B^0 \rightarrow K^0e^\pm\mu^\mp$	$1.1^{+2.1}_{-0.9}$	4.1	0.5	14.6	± 7.3	± 11.2	$0.9^{+1.9}_{-0.8}$	4.1
$B^+ \rightarrow K^{*+}e^\pm\mu^\mp$	$-0.4^{+1.8}_{-0.0}$	3.5	1.1	9.3	± 9.6	± 3.0	$-0.8^{+3.8}_{-0.0}$	8.0

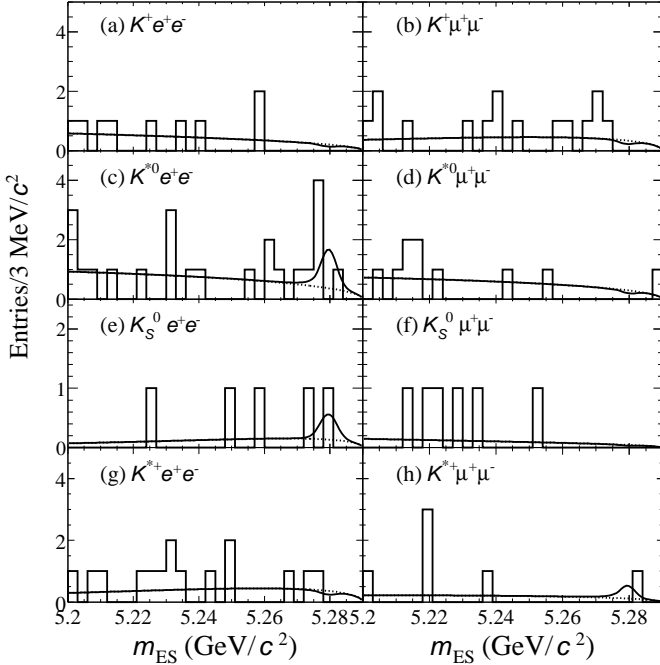


FIG. 3: Projections from individual maximum likelihood fits onto m_{ES} for the ΔE signal regions: $-0.11 < \Delta E < 0.05$ GeV (electrons) and $-0.07 < \Delta E < 0.05$ GeV (muons). The dotted lines show the background component, and the solid lines show the sum of background and signal components.

The systematic uncertainties on the efficiency, $(\Delta\mathcal{B}/\mathcal{B})_\epsilon$, are listed in Table I and arise from charged-particle tracking ($\pm 1.2\%$ /lepton, $\pm 2.0\%$ for the pion from $K^* \rightarrow K\pi$, and $\pm 1.3\%$ /track for other charged hadrons), particle identification ($\pm 1.4\%$ /electron, $\pm 1.0\%$ /muon, $\pm 2.0\%$ /track for kaons and pions), the continuum sup-

pression cut ($\pm 2.0\%$), the $B\bar{B}$ suppression cut ($\pm 3.0\%$), K_S^0 selection ($\pm 4.0\%$), Monte Carlo signal statistics ($\pm 3.0\%$ to $\pm 5.0\%$), the theoretical model dependence of the efficiency ($\pm 4.0\%$ to $\pm 7.0\%$, depending on the mode), and the number of $B\bar{B}$ events ($\pm 1.6\%$). The uncertainties on the efficiencies due to model-dependence of form factors are taken to be the full range of variation obtained from different theoretical models [1]. In setting an upper limit, the systematic uncertainties from the efficiency, $(\Delta\mathcal{B}/\mathcal{B})_\epsilon$, and from the fit, $(\Delta\mathcal{B}/\mathcal{B})_{\text{fit}}$, are added in quadrature, and the limit is increased by this factor.

Table I also includes the results for the lepton-family-violating decays $B \rightarrow K^{(*)}e\mu$, where the signal efficiencies were determined from phase-space Monte Carlo simulations. We observe no evidence for these decays.

We determine the branching fractions $\mathcal{B}(B \rightarrow K\ell^+\ell^-)$ and $\mathcal{B}(B \rightarrow K^*\ell^+\ell^-)$ averaged over both B meson charge and lepton type (e^+e^- and $\mu^+\mu^-$) by performing a simultaneous maximum likelihood fit to the four contributing channels in each case. In combining the $B \rightarrow K^*\ell^+\ell^-$ modes, the ratio of branching fractions $\mathcal{B}(B \rightarrow K^*e^+e^-)/\mathcal{B}(B \rightarrow K^*\mu^+\mu^-) = 1.2$ from the model of Ali *et al.* [1] is used to weight the yield in the muon channel relative to that in the electron channel. The extracted yield corresponds to the electron mode. The combined fits give

$$\begin{aligned}\mathcal{B}(B \rightarrow K\ell^+\ell^-) &= (-0.06^{+0.24}_{-0.00} \pm 0.03) \times 10^{-6}, \\ \mathcal{B}(B \rightarrow K^*\ell^+\ell^-) &= (0.9^{+1.3}_{-0.9} \pm 0.1) \times 10^{-6},\end{aligned}$$

where the first error is statistical and the second is systematic. We evaluate the upper limits on these combined modes and obtain

$$\begin{aligned}\mathcal{B}(B \rightarrow K\ell^+\ell^-) &< 0.50 \times 10^{-6} \text{ at } 90\% \text{ C.L.} \\ \mathcal{B}(B \rightarrow K^*\ell^+\ell^-) &< 2.9 \times 10^{-6} \text{ at } 90\% \text{ C.L.}\end{aligned}$$

These limits represent an improvement over previously published results from CDF [11] and CLEO [12]. The Belle [13] experiment has also recently obtained results on these modes. We see no evidence for a signal, and our limits are close to many of the predictions based on the Standard Model. With the rapidly increasing size of our data sample, we expect to have significantly better sensitivity to these modes in the future.

We are grateful for the excellent luminosity and machine conditions provided by our PEP-II colleagues. The collaborating institutions wish to thank SLAC for its support and kind hospitality. This work is supported by DOE and NSF (USA), NSERC (Canada), IHEP (China), CEA and CNRS-IN2P3 (France), BMBF (Germany), INFN (Italy), NFR (Norway), MIST (Russia), and PPARC (United Kingdom). Individuals have received support from the Swiss NSF, A. P. Sloan Foundation, Research Corporation, and Alexander von Humboldt Foundation.

* Also with Università di Perugia, Perugia, Italy

† Also with Università della Basilicata, Potenza, Italy

- [1] A. Ali *et al.*, Phys. Rev. D **61**, 074024 (2000); P. Colangelo *et al.*, Phys. Rev. D **53**, 3672 (1996); D. Melikhov, N. Nikitin, and S. Simula, Phys. Rev. D **57**, 6814 (1998).
- [2] T.M. Aliev *et al.*, Phys. Lett. B **400**, 194 (1997); T.M. Aliev, M. Savci, and A. Özpineci, Phys. Rev. D **56**, 4260 (1997); G. Burdman, Phys. Rev. D **52**,

6400 (1995); C. Greub, A. Ioannissian, and D. Wyler, Phys. Lett. B **346**, 149 (1995); J.L. Hewett and J.D. Wells, Phys. Rev. D **55**, 5549 (1997); C.Q. Geng and C.P. Kao, Phys. Rev. D **54**, 5636 (1996); and references therein.

- [3] CLEO Collaboration, R. Ammar *et al.*, Phys. Rev. Lett. **71**, 674 (1993).
- [4] CLEO Collaboration, M.S. Alam *et al.*, Phys. Rev. Lett. **74**, 2885 (1995).
- [5] BABAR Collaboration, B. Aubert *et al.*, hep-ex/0105044, to appear in Nucl. Instrum. Methods (2001).
- [6] G.C. Fox and S. Wolfram, Phys. Rev. Lett. **41**, 1581 (1978).
- [7] R.A. Fisher, Ann. Eugenics **7**, 179 (1936).
- [8] “GEANT–Detector Description and Simulation Tool”, CERN Program Library Long Writeup W5013 (1995).
- [9] We parametrize the background shape using

$$f(m_{\text{ES}}, \Delta E) = N e^{-s\Delta E} m_{\text{ES}} \sqrt{1 - \frac{m_{\text{ES}}^2}{E_b^{*2}}} e^{-\xi \left(1 - \frac{m_{\text{ES}}^2}{E_b^{*2}}\right)},$$

where N is a normalization factor and s and ξ are free parameters determined from the fit to the data.

- [10] Whenever possible, we report two-sided 68% central confidence intervals. For channels constrained by the requirement that the total fit function be non-negative, we quote a single-sided 68% confidence interval and set the lower statistical error to zero.
- [11] CDF Collaboration, T. Affolder *et al.*, Phys. Rev. Lett. **83**, 3378 (1999).
- [12] CLEO Collaboration, S. Anderson *et al.*, Phys. Rev. Lett. **87**, 181803 (2001).
- [13] Belle Collaboration, K. Abe *et al.*, hep-ex/0109026, submitted to Phys. Rev. Lett.